

# Liquid–Liquid Equilibria of Nitrobenzene–Inorganic Acid Systems at 298.15 K

K. R. Suresh, P. Ghosh, and T. Banerjee\*

Department of Chemical Engineering, Indian Institute of Technology Guwahati, Guwahati 781039, Assam, India

Liquid–liquid equilibria (LLE) of nitrobenzene–sulfuric acid–water and nitrobenzene–nitric acid–water systems were experimentally determined at 298.15 K. The NRTL and UNIQUAC models were used to correlate the experimental data. The fit of these models to the experimental data were very good, and the root-mean-square deviations for both the systems were found to be less than 1 %. It was observed that the solubility of both acids in the organic phase and the solubility of nitrobenzene in the aqueous phase increased with the increase in concentration of acid in the mixture.

## Introduction

Several industrial reactions involve heterogeneous liquid–liquid systems where an organic compound reacts with one or more mineral acids (such as sulfuric and nitric acids). An example of wide commercial importance is the nitration of aromatic compounds by mixed acid (a mixture of concentrated sulfuric and nitric acids). This reaction takes place by the transfer of the organic compound into the aqueous phase where the nitronium ion exists. The concentration of sulfuric acid is important in this transfer, which consequently influences the overall rate of reaction and the yield of the product. To date, there has been hardly any study on the phase equilibria involving organic compounds, sulfuric acid, and nitric acid, probably due to the fact that in many such systems the organic compound undergoes spontaneous sulfonation or nitration.

The analysis of liquid–liquid equilibrium (LLE) involves the use of the excess Gibbs free energy models such as NRTL<sup>1</sup> and UNIQUAC<sup>2</sup> to correlate the tie line data. These models use activity coefficients, which require appropriate binary interaction parameters, which can represent the LLE for highly nonideal liquid mixtures. In the present work, our objective was to generate the ternary LLE of nitrobenzene–sulfuric acid–water and nitrobenzene–nitric acid–water systems and correlate the tie line data by the NRTL and UNIQUAC models.

## Experimental

**Chemicals.** Nitrobenzene (99 % purity), sulfuric acid (98 % w/w), and nitric acid (70 % w/w) were procured from Merck (India). Nitric acid (100 % w/w) was procured from Merck (Germany). The Karl Fischer reagent (pyridine-free, 99 % purity) was procured from Merck (India). Dry methanol (99.5 % purity), oxalic acid (99 % purity), sodium hydroxide (98 % purity), acetone (99 % purity), methanol (HPLC grade), and acetonitrile (HPLC grade) were also procured from Merck (India). Standard samples of 1,3-dinitrobenzene (97 % purity) and 1,3-nitrobenzenesulfonic acid (sodium salt, 98 % purity) were procured from Alfa Aesar (India). The water used in this study was purified from a Millipore water purification system. Its conductivity was  $1 \cdot 10^{-7} \Omega^{-1} \text{ cm}^{-1}$ , and its surface tension was  $72.5 \text{ mN} \cdot \text{m}^{-1}$  (298.15 K). Sulfuric acid solutions of lower concentration were prepared by diluting the 98

% acid with water. Nitric acid solutions of intermediate concentrations (i.e., between 70 % and 100 %) were prepared by diluting the 100 % acid.

**Equilibrium Measurements.** To generate the tie line data for the ternary phase diagrams, several compositions were chosen such that the mixtures developed heterogeneity. The heterogeneous mixtures of nitrobenzene and aqueous acid solutions were agitated for approximately 4 h in sealed glass vessels placed inside a water bath under magnetic stirring. The equilibrated mixtures were allowed to separate into two phases for one day in separating funnels. The aqueous and organic phases were analyzed as follows. Samples from the aqueous phase (about 1 g) were collected and dissolved in methanol. The amount of nitrobenzene present in the sample was determined by its absorption at  $\lambda_{\text{max}} = 260 \text{ nm}$  using a UV–visible spectrophotometer (make: Perkin-Elmer, model: lambda 35). The amounts of sulfuric (or nitric) acid present in the aqueous and organic phases were determined by acid–base titration using aqueous NaOH solutions, which were standardized with standard aqueous oxalic acid solutions. The amount of water present in the aqueous phase was calculated by material balance. The amount of water present in the organic phase was determined by Karl Fischer titration. The amount of nitrobenzene present in the organic phase was calculated by material balance.

The possibility of formation of 1,3-nitrobenzenesulfonic acid was investigated by HPLC [make: Perkin-Elmer, model: series 200, column: Merck Hibar-Purospher RP-18, detector: UV,  $\lambda = 254 \text{ nm}$ ]. The mobile phase was constituted of acetonitrile and water in a 4:1 volumetric ratio. The possibility of formation of 1,3-dinitrobenzene was investigated by Janovsky's test<sup>3</sup> using the UV–visible spectrophotometer at  $\lambda_{\text{max}} = 570 \text{ nm}$ . It was found that neither 1,3-nitrobenzenesulphonic acid nor 1,3-dinitrobenzene formed at room temperature. However, at higher temperatures (e.g., 313.15 K and above), nitrobenzene underwent sulfonation as well as nitration at high concentrations (e.g., > 75 %) of the respective acids.

The experimental data were reproducible. We repeated the experiments three times and obtained results which deviated from one another within  $\pm 5 \%$ . All experiments were conducted at room temperature (298.15 K).

## Results and Discussion

**Tie Line Correlation.** The electrolyte–NRTL model<sup>4,5</sup> can be used to correlate the experimental data on phase equilibria of ionic

\* Author to whom all correspondence should be addressed. E-mail: tamalb@iitg.ernet.in. Tel.: +91.361.2582266. Fax: +91.361.2690762.

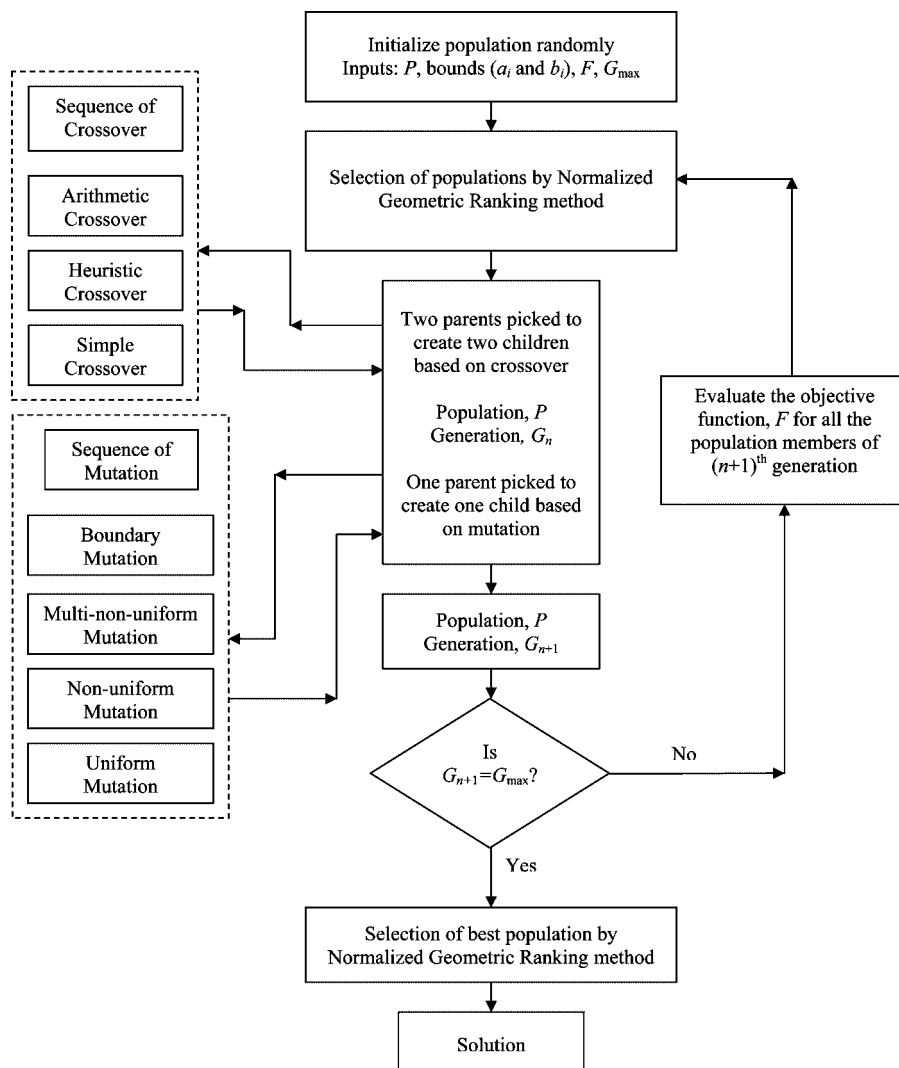


Figure 1. Flow diagram for float genetic algorithm (FGA).<sup>13,14</sup>

species. Recently, the electrolyte–NRTL model has been applied to weak electrolytes such as ionic liquids.<sup>6</sup> A few other models have been developed using the Wilson equation<sup>7</sup> and the UNIQUAC model,<sup>8,9</sup> which have accounted for the local compositions and short-range forces. To compare these models with experimental data, one must relate the ionic activity coefficients to the mean activity coefficient of the electrolyte in the solution, which is the quantity actually measured. The electrolyte can be either completely or partially dissociated. In the latter case, Chen’s model<sup>5</sup> can be used, albeit with a constraint.

In these models, the chemical equilibrium constant for dissociation was used as an adjustable parameter. The equilibrium constant was assumed not to vary with composition. However, for the systems used in the present study, the equilibrium constants vary with composition.<sup>10</sup> Since each tie line in the ternary diagram represents a particular composition, the equilibrium constant varies for each tie line. Another aspect of concern was the effect of nitrobenzene on the dissociation of the acids, which is unknown. It has been reported in the literature that nitrobenzene lowers the acidity of sulfuric acid significantly.<sup>11</sup>

The dissociation of sulfuric acid in aqueous solution occurs in two steps. In the first step, it dissociates into a hydrogen sulfate ion ( $\text{HSO}_4^-$ ) and a proton, which combines with water to form the hydroxonium ion ( $\text{H}_3\text{O}^+$ ). The hydrogen sulfate ion is a very weak conjugate base. However, it can act as an acid (a weak one)

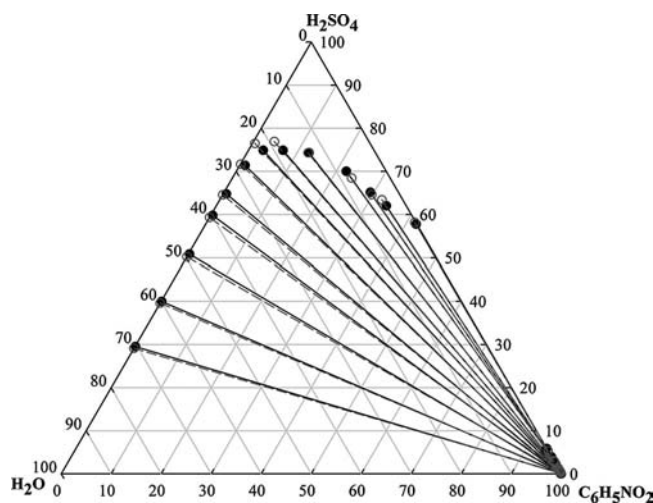


Figure 2. Experimental and NRTL-predicted tie lines for the nitrobenzene–sulfuric acid–water system at 298.15 K. ●, Experimental; ○, NRTL prediction.

not nearly as strong as sulfuric acid. Since the hydrogen sulfate ion is not a very strong acid, only a small amount of  $\text{H}_3\text{O}^+$  is produced from its dissociation. In aqueous solution, the relative amounts of  $\text{HSO}_4^-$  and  $\text{SO}_4^{2-}$  depend upon the concentration of sulfuric acid. For example, the amount of  $\text{HSO}_4^-$  increases from

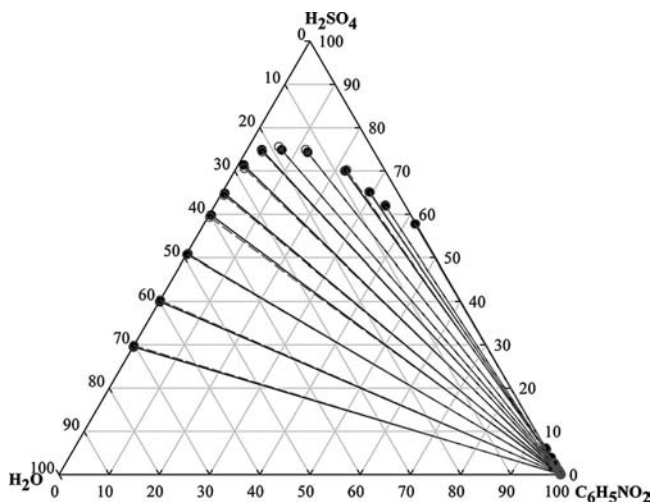


Figure 3. Experimental and UNIQUAC-predicted tie lines for the nitrobenzene–sulfuric acid–water system at 298.15 K. ●, Experimental; ○, UNIQUAC prediction.

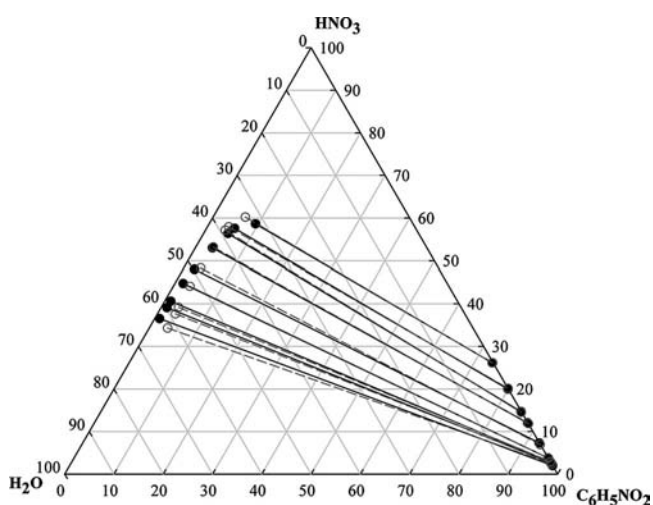


Figure 4. Experimental and NRTL-predicted tie lines for the nitrobenzene–nitric acid–water system at 298.15 K. ●, Experimental; ○, NRTL prediction.

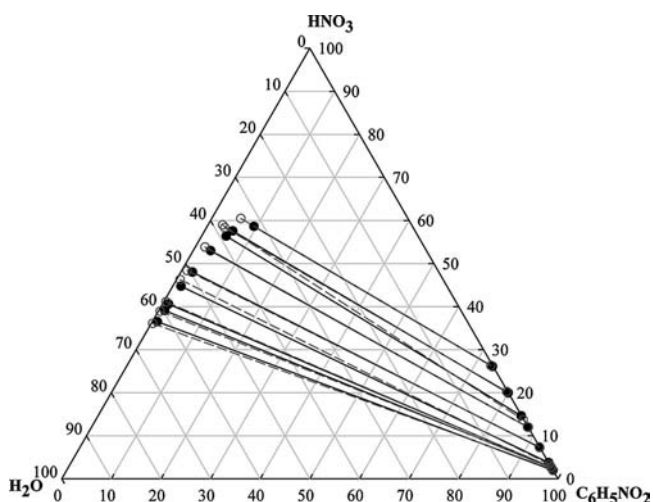


Figure 5. Experimental and UNIQUAC-predicted tie lines for the nitrobenzene–nitric acid–water system at 298.15 K. ●, Experimental; ○, UNIQUAC prediction.

67 % in  $0.1 \text{ mol} \cdot \text{dm}^{-3}$  aqueous solution to 95 % in  $13 \text{ mol} \cdot \text{dm}^{-3}$  solution. At higher concentrations, the amount of undissociated sulfuric acid becomes significant.<sup>10</sup> A recent molecular dynamics

simulation has reported similar variations.<sup>12</sup> To alleviate these difficulties, the correlations of LLE were carried out using the conventional NRTL and UNIQUAC models.<sup>1,2</sup>

According to the NRTL model, the nonideal liquid phase activity coefficient ( $\gamma$ ) of component  $i$  is given by the following equation.<sup>1</sup>

$$\ln \gamma_i = \frac{\sum_{j=1}^c \tau_{ji} G_{ji} x_j}{\sum_{k=1}^c G_{ki} x_k} + \sum_{j=1}^c \left[ \frac{G_{ij} x_j}{\sum_{k=1}^c G_{kj} x_k} \left( \tau_{ij} - \frac{\sum_{i=1}^c \tau_{ij} G_{ij} x_i}{\sum_{k=1}^c G_{kj} x_k} \right) \right] \quad (1)$$

where

$$G_{ji} = \exp(-\alpha_{ji} \tau_{ji}) \quad (2)$$

The UNIQUAC model gives the following equation for the nonideal activity coefficient for component  $i$ .<sup>2</sup>

$$\ln \gamma_i = \ln \left( \frac{\Phi_i}{x_i} \right) + \frac{z}{2} q_i \ln \left( \frac{\theta_i}{\Phi_i} \right) + l_i - \frac{\Phi_i}{x_i} \sum_{j=1}^c x_j l_j + q_i \left( 1 - \ln \sum_{j=1}^c \theta_j \tau_{ji} - \sum_{j=1}^c \frac{\theta_j \tau_{ij}}{\sum_{k=1}^c \theta_k \tau_{kj}} \right) \quad (3)$$

where

$$\tau_{ji} = \frac{g_{ji} - g_{ii}}{RT} = \frac{A_{ji}}{T} \quad (4)$$

$$\theta_i = \frac{q_i x_i}{q_T} \quad (5)$$

$$q_T = \sum_k q_k x_k \quad (6)$$

$$\Phi_i = \frac{r_i x_i}{r_T} \quad (7)$$

$$r_T = \sum_k r_k x_k \quad (8)$$

$$l_i = \frac{z}{2} (r_k - q_k) + 1 - r_k \quad (9)$$

In eqs 1 to 9,  $\theta$ ,  $\tau$ , and  $\Phi$  represent the area fraction, interaction parameter, and segment fraction, respectively. The pure-component surface area parameter and the pure-component volume parameter in the UNIQUAC model are represented by  $r$  and  $q$ , respectively. The mole fraction in the liquid phase is represented by  $x$ , and the coordination number is represented by  $z (= 10)$ . We have used  $\alpha_{ij} = \alpha_{ji} = 0.2$  in our calculations. In eq 4,  $g_{ji}$  represents the average interaction energy for the interaction of molecules of component  $j$  with molecules of

**Table 1. Experimental Tie Line Data, Selectivities, and Distribution Ratios Measured for the Two Systems at  $T = 298.15$  K**

System: Nitrobenzene–Sulfuric Acid–Water								
Sl. No.	aqueous phase (wt. fraction)			organic phase (wt. fraction)			$D_2$	$S$
	$C_6H_5NO_2$	$H_2SO_4$	$H_2O$	$C_6H_5NO_2$	$H_2SO_4$	$H_2O$		
01	0.001	0.295	0.704	0.999	0.001	0.000	0.003	294705
02	0.001	0.400	0.599	0.999	0.001	0.000	0.003	399600
03	0.002	0.508	0.489	0.999	0.000	0.001	0.000	-
04	0.004	0.598	0.398	0.999	0.000	0.001	0.000	-
05	0.006	0.648	0.346	1.000	0.000	0.000	0.000	-
06	0.011	0.714	0.275	0.999	0.001	0.000	0.001	64844
07	0.030	0.749	0.222	0.996	0.003	0.000	0.004	8289
08	0.069	0.749	0.182	0.992	0.007	0.000	0.009	1538
09	0.124	0.743	0.133	0.990	0.010	0.000	0.013	593
10	0.220	0.700	0.080	0.960	0.039	0.000	0.056	78
11	0.293	0.651	0.056	0.973	0.026	0.000	0.040	83
12	0.340	0.620	0.040	0.974	0.023	0.000	0.037	77
13	0.421	0.578	0.002	0.941	0.059	0.001	0.102	22

System: Nitrobenzene–Nitric Acid–Water								
Sl. No.	aqueous phase (wt. fraction)			organic phase (wt. fraction)			$D_2$	$S$
	$C_6H_5NO_2$	$HNO_3$	$H_2O$	$C_6H_5NO_2$	$HNO_3$	$H_2O$		
01	0.010	0.365	0.625	0.980	0.020	0.000	0.055	1789
02	0.012	0.391	0.597	0.973	0.026	0.001	0.066	1219
03	0.012	0.406	0.582	0.972	0.027	0.000	0.067	1218
04	0.017	0.447	0.536	0.962	0.038	0.000	0.085	666
05	0.023	0.480	0.497	0.926	0.073	0.001	0.152	265
06	0.035	0.530	0.435	0.879	0.120	0.001	0.226	111
07	0.049	0.564	0.387	0.853	0.146	0.001	0.259	67
08	0.057	0.576	0.368	0.800	0.200	0.001	0.347	40
09	0.094	0.586	0.320	0.737	0.261	0.002	0.445	18

**Table 2. NRTL and UNIQUAC Interaction Parameters for the Two Systems at  $T = 298.15$  K**

$i-j$	NRTL model parameters				UNIQUAC model parameters			
	$A_{ij}/K$	$A_{ji}/K$	$F^a$	rmsd <sup>a</sup>	$A_{ij}/K$	$A_{ji}/K$	$F^a$	rmsd <sup>a</sup>
System: Nitrobenzene (1)–Sulfuric Acid (2)–Water (3)								
1–2	3.237	8.212	$2.16 \cdot 10^{-3}$	0.526	769.48	-20.694	$9.6 \cdot 10^{-4}$	0.356
1–3	11.251	19.960			590.43	-121.810		
2–3	14.739	15.198			-940.47	-10.151		
System: Nitrobenzene (1)–Nitric Acid (2)–Water (3)								
1–2	2.206	17.738	$4.37 \cdot 10^{-3}$	0.906	649.44	-61.217	$3.33 \cdot 10^{-3}$	0.654
1–3	17.836	3.623			999.94	999.520		
2–3	10.339	19.950			996.90	-374.130		

<sup>a</sup>  $F$  and rmsd were calculated from eqs 10 and 11, respectively.

component  $i$ ;  $R$  represents the gas constant; and  $T$  represents the temperature.

**Genetic Algorithm.** GA was first proposed by Holland<sup>13</sup> and has been widely used in recent times. It is a method that searches for the global optima of an objective function through the use of simulated evolution: the survival of the fittest strategy. Unlike most of the optimization methods, GA does not require any initial guess but only the upper and lower bounds of the variables, i.e., the interaction parameters in the present work. GA explores all regions of the solution space and exponentially exploits the promising areas through selection: crossover and mutation operations applied to the interaction parameters in the population. Float genetic algorithm (FGA) is better than both binary genetic algorithm (BGA) and simulated annealing in terms of computational efficiency and solution quality.<sup>14</sup> FGA has been used for the estimation of interaction parameters in the present work. It shows an improved predicted phase envelope and good agreement with the experimental data.<sup>15</sup>

The flow diagram for FGA is given in Figure 1. FGA starts with initial populations of fixed size. Interaction parameters in the initial populations are generated randomly. Normalized geometric ranking (a probabilistic selection method) is used for the selection of populations. This method selects populations for the next generation based on their fitness to the objective

function. This is the role played by the probability of selecting the best individual ( $q$ ). Remainder populations are randomly generated. The size of the population remains the same in each generation. New populations are generated, each generation using genetic operators: crossover (arithmetic, heuristic, and simple) and mutation (boundary, multinon-uniform, nonuniform, and uniform). GA moves from generation to generation until a termination criterion is met. The most frequently used stopping criterion is a specified maximum number of generations ( $G_{max}$ ).<sup>14,15</sup> Finally, GA gives the best population of interaction parameters, which is available at the top of the list as organized by the ranking method from the final generation as the required solution.

The experimental data obtained for both the systems are presented in Table 1. The binary interaction parameters were obtained from the experimental LLE data by minimizing the objective function, which was defined as the sum of the square of errors between the experimental and calculated compositions of all the components over the entire set of tie lines [as per eq 10]. The methodology, application, and details were presented in our earlier work.<sup>15</sup> We have taken the population size,  $n_{pop} = 100$ , and the number of generations,  $n_{gen} = 200$ , for the GA program. As the GA toolbox<sup>14</sup> in MATLAB is for maximization, the objective function ( $F$ ) for

minimizing the total error between the experimental and calculated mole fractions was defined as

$$\text{Maximize: } F_{(\text{with respect to } A_{ij} \text{ where } i,j=1,2,3 \text{ and } j \neq i)} = - \sum_{k=1}^m \sum_{l=1}^n \sum_{i=1}^c w_{ik}^l (x_{ik}^l - \hat{x}_{ik}^l)^2, w_{ik}^l = 1 \quad (10)$$

The goodness of the fit was measured by the root-mean-square deviation (rmsd) defined as

$$\text{RMSD (in \%)} = \left( \frac{F}{2mc} \right)^{1/2} = \left[ \sum_{k=1}^m \sum_{i=1}^c \sum_{l=1}^n \frac{(x_{ik}^l - \hat{x}_{ik}^l)^2}{2mc} \right]^{1/2} \cdot 100 \quad (11)$$

where  $m$  refers to the number of tie lines and  $c$  refers to the number of components (viz., three for the present systems). Here  $x_{ik}^l$  and  $\hat{x}_{ik}^l$  are the experimental and predicted values of composition (in mole fraction) for component  $i$  for the  $k^{\text{th}}$  tie line in phase  $l$ , respectively. The modified Rachford–Rice algorithm<sup>16</sup> was used for the calculation of the tie lines. For the UNIQUAC model, the structure parameters  $r$  and  $q$  of the acids were predicted using the Polarizable Continuum Model (PCM) as outlined in our previous work.<sup>17</sup> The values of  $r = 3.229$  and  $q = 1.713$  for sulfuric acid, and  $r = 2.339$  and  $q = 1.398$  for nitric acid were used for regressing the data using the UNIQUAC model.

The tie lines predicted by NRTL and UNIQUAC models are compared with the experimental tie lines in Figures 2 and 3 for sulfuric acid and Figures 4 and 5 for nitric acid, respectively. The NRTL and UNIQUAC interaction parameters are presented in Table 2. The rmsd for the sulfuric acid system was obtained as 0.5 % and 0.4 % for NRTL and UNIQUAC models, respectively. The rmsd values of 0.9 % and 0.7 % were obtained for the nitric acid system using these models. These results show that the application of the NRTL and UNIQUAC models along with GA fitted the experimental data very accurately.

**Interpretation of the Tie Line Behavior.** The distribution of acid between the aqueous and organic phases was determined from the following equation.

$$D_2 = \left( \frac{w_a^{\text{org}}}{w_a^{\text{aq}}} \right) \quad (12)$$

The selectivity indicating the separation of nitrobenzene and acid by water was defined as

$$S = \frac{\left( \frac{w_{\text{NB}}^{\text{org}}}{w_{\text{NB}}^{\text{aq}}} \right)}{\left( \frac{w_a^{\text{org}}}{w_a^{\text{aq}}} \right)} \quad (13)$$

Here  $w_a^{\text{aq}}$  and  $w_a^{\text{org}}$  indicate the weight fractions of acid in the aqueous and organic phases, respectively, while  $w_{\text{NB}}^{\text{aq}}$  and  $w_{\text{NB}}^{\text{org}}$  represent the weight fractions of nitrobenzene in the aqueous and organic phases, respectively. The values of solute distribution coefficient  $D_2$  and selectivity  $S$  are shown in Figures 6 to

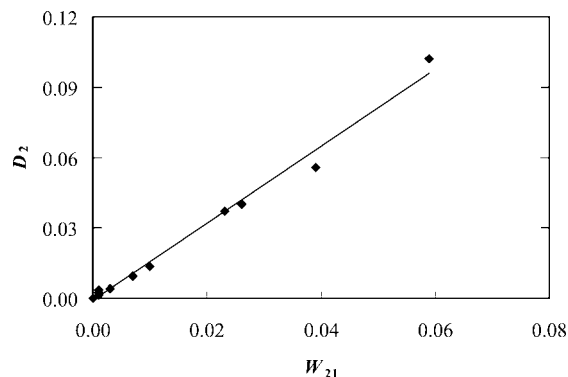


**Figure 6.** Solute distribution coefficient ( $D_2$ ) as a function of the weight fraction of sulfuric acid in the organic phase ( $W_{21}$ ). Coefficient of determination ( $R^2$ ) = 0.9897.

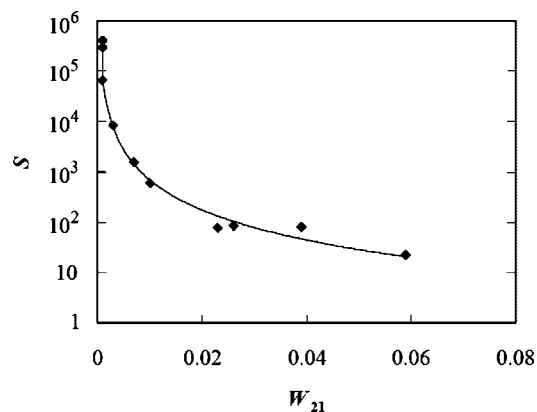


**Figure 7.** Selectivity ( $S$ ) as a function of the weight fraction of sulfuric acid in the organic phase ( $W_{21}$ ).

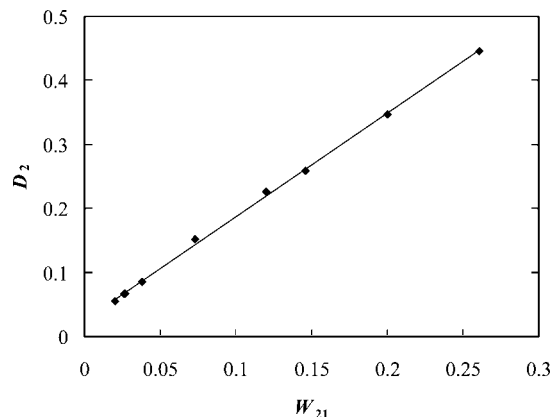


**Figure 8.** Solute distribution coefficient ( $D_2$ ) as a function of the weight fraction of nitric acid in the organic phase ( $W_{21}$ ). Coefficient of determination ( $R^2$ ) = 0.999.

9 for both the systems. The solute distribution coefficient  $D_2$  increased linearly with the increase in weight fraction of acid in the organic phase  $W_{21}$  ( $\equiv w_a^{\text{org}}$ ). The weight fraction of acid in the organic phase was always much smaller than that in the aqueous phase. At the same time, the weight fraction of acid in the aqueous phase varied within a rather small range as compared to its variation in the organic phase. That is the reason why  $D_2$  decreased with increase in  $W_{21}$  linearly. However, the selectivity  $S$  decreased nonlinearly with  $W_{21}$ . This observation can be explained by the fact that the solubility of the acid in the organic phase and the solubility of nitrobenzene in the aqueous phase increased with the increase in concentration of acid in the mixture.

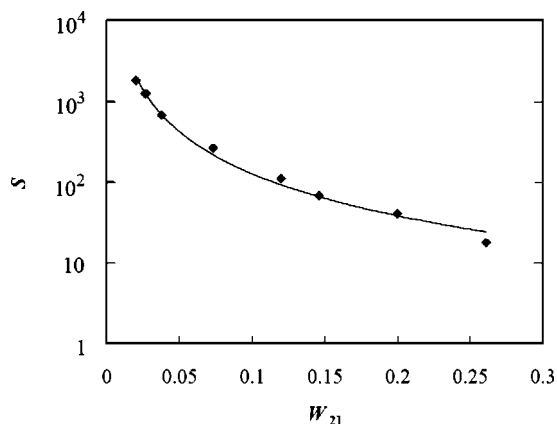


**Figure 9.** Selectivity ( $S$ ) as a function of the weight fraction of nitric acid in the organic phase ( $W_{21}$ ).

### Conclusion

The experimental ternary liquid–liquid equilibria of nitrobenzene–sulfuric acid–water and nitrobenzene–nitric acid–water systems were fitted well by the NRTL and UNIQUAC models with  $\text{rmsd} < 1\%$ . The distribution coefficients of the acids increased with their concentration in the organic phase. The selectivity reduced with the concentration of the acids in the organic phase.

### Literature Cited

- (1) Renon, H.; Prausnitz, J. M. Local Compositions in Thermodynamic Excess Functions for Liquid Mixtures. *AIChE J.* **1968**, *14*, 135–144.
- (2) Abrams, D. S.; Prausnitz, J. M. Statistical Thermodynamics of Liquid Mixtures. New Expression for the Excess Gibbs Energy of Partly or Completely Miscible Systems. *AIChE J.* **1975**, *21*, 116–128.
- (3) Urbanski, T. *Chemistry and Technology of Explosives*; Pergamon: New York, 1987.
- (4) Chen, C. C.; Evans, B. B. A Local Composition Model for the Excess Gibbs Energy of Aqueous Electrolyte Systems. *AIChE J.* **1986**, *32*, 444–454.
- (5) Chen, C. C.; Bokis, C. P.; Mathias, P. Segment-Based Excess Gibbs Energy Model for Aqueous Organic Electrolytes. *AIChE J.* **2001**, *47*, 2593–2602.
- (6) Belvéze, S. L.; Brennecke, J. F.; Stadther, M. A. Modeling of Activity Coefficients of Aqueous Solutions of Quaternary Ammonium Salts with the Electrolyte-NRTL Equation. *Ind. Eng. Chem. Res.* **2004**, *43*, 815–825.
- (7) Liu, Y.; Harvey, A. H.; Prausnitz, J. M. Thermodynamics of Concentrated Electrolyte Solutions. *Chem. Eng. Commun.* **1989**, *77*, 43–66.
- (8) Sander, B.; Rasmussen, P.; Fredenslund, A. Calculation of Vapour-Liquid Equilibria in Nitric Acid-Water-Nitrate Salt Systems Using an Extended UNIQUAC Equation. *Chem. Eng. Sci.* **1986**, *41*, 1185–1195.
- (9) Sander, B.; Rasmussen, P.; Fredenslund, A. Calculation of Solid-Liquid Equilibria in Aqueous Solutions of Nitrate Salts Using an Extended UNIQUAC Equation. *Chem. Eng. Sci.* **1986**, *41*, 1197–1202.
- (10) Robertson, E. B.; Dunford, H. B. The State of the Proton in Aqueous Sulfuric Acid. *J. Am. Chem. Soc.* **1964**, *86*, 5080–5089.
- (11) Westheimer, F. H.; Kharasch, M. S. The Kinetics of Nitration of Aromatic Nitro Compounds in Sulfuric Acid. *J. Am. Chem. Soc.* **1946**, *68*, 1871–1876.
- (12) Choe, Y. K.; Tsuchida, E.; Ikeshoji, T. First-Principles Molecular Dynamics Study on Aqueous Sulfuric Acid Solutions. *J. Chem. Phys.* **2007**, *126*, 154510–154519.
- (13) Holland, J. H. *Adaptation in Natural and Artificial Systems*; The University of Michigan Press: Ann Arbor, 1975.
- (14) Houck, C. R.; Joines, J. A.; Kay, M. G. NCSU-IE TR 95–09, 1995. (URL: [www.ie.ncsu.edu/mirage/GAToolBox/gaot/](http://www.ie.ncsu.edu/mirage/GAToolBox/gaot/)).
- (15) Banerjee, T.; Singh, M. K.; Sahoo, K. R.; Khanna, A. Genetic Algorithm to Estimate Interaction Parameters of Multicomponent Systems for Liquid-Liquid Equilibria. *Comp. Chem. Eng.* **2005**, *29*, 1712–1719.
- (16) Seader, J. D.; Henley, E. J. *Separation Process Principles*; Wiley: New York, 1998.
- (17) Banerjee, T.; Singh, M. K.; Sahoo, K. R.; Khanna, A. Volume, Surface and UNIQUAC Interaction Parameters for Imidazolium Based Ionic Liquids via Polarizable Continuum Model. *Fluid Phase Equilib.* **2005**, *234*, 64–76.

Received for review November 19, 2008. Accepted January 25, 2009. The work reported in this article was financially supported by a research grant [No. 01(2123)/07/EMR-II] from the Council of Scientific and Industrial Research (CSIR), Government of India.

JE800878B